
©2009 IEEE. Personal use of this material is permitted. However, permission to reprint/republish this material for advertising or promotional purposes or for creating new collective works for resale or redistribution to servers or lists, or to reuse any copyrighted component of this work in other works must be obtained from the IEEE.

Integration of Plug-In Hybrid Electric Vehicles into Energy Networks

Matthias D. Galus *Student Member, IEEE*, Göran Andersson, *Fellow, IEEE*

Abstract—Electrification of substantial percentages of individual transportation through Plug-In Hybrid Electric Vehicles (PHEVs) will lead to an integration of power and transport systems. This, in turn, will impose an additional demand on today’s power system, potentially stressing hazardous for some pieces of equipment. Smart management schemes, investigated in this paper, can alleviate possible congestion issues in power systems by intelligently distributing available energy among connected PHEVs, modelled as agents with individual parameters and goals. The management scheme is integrated in aggregation entities, clustering PHEVs in various urban areas. Network impacts resulting from the smart management scheme will be studied based on power flow calculations. The analysis will give implications for PHEV integration schemes as well as tentative ideas of possible repercussions on hybrid power systems and how to counteract.

Index Terms—Plug-In Hybrid Electric Vehicles (PHEV), Energy Hub Networks, Agent Based Modelling, Demand Management, Load Shedding

I. INTRODUCTION

The preceding scarcity of crude oil, growing CO₂ emissions and other factors initiated a “green” economy, resulting partly in the strive for more efficient individual transportation. Plug In Hybrid Electric Vehicles (PHEV) show the potential for substantial electrification of the individual transportation sector [1]. Almost solely running on batteries until depletion, the vehicles can be recharged via their plug to maintain high efficiency operation but also use a combustion engine as an auxiliary power source. Clearly, in the short term they will become an electric load [2], [3] but the amalgamation promises also many advantages to electricity networks. Some of which would be the introduction of a large, controllable load or of a storage for renewable generation expansion [4], [5].

Before being able to manage the advantages of this upcoming technology, system impacts need to be studied, assuring sustainability of electricity networks. Therefore, PHEVs have to be first considered as mobile loads, implying new load patterns. Past studies dealt with utility impacts and results are suggesting that the current power generation capacity in some countries is able to supply the additional load even incorporating specific underlying assumptions on time dependence [4], [6]. For the most part, night time charging is presumed and only minor recharging is undertaken during the day. Also, utility controlled recharging is found to result in improved load duration curves. Only recently, system constraints implied by the grid, distribution grids in specific, are moving into the focus of researchers [7]–[9].

M.D. Galus and G. Andersson are with the Power Systems Laboratory, Swiss Federal Institute of Technology (ETH) Zurich, Switzerland. Corresponding author’s email address galus@eeh.ee.ethz.ch

The focus of this paper is to introduce a general integration scheme for PHEV into power networks, which are modelled by the energy hub concept. Hence, possible, technical network limitations are taken into account. Models from power systems will be used to represent the networks and a decentralized PHEV management scheme [10] will be introduced for several nodes in the network. The system shows the ability to study impacts with and without an additional central network management scheme, supervising managers, ensuring system security and enabling conclusions on system ramifications. Utilizing this general approach renders the disquisition on effects not only limited to the electricity network as gas is included. The approach incorporates the advantage of being easily scalable, specifically down for electricity systems, only.

In the next sections, the energy hub concept will shortly be delineated, the PHEV model will be introduced and the integration scheme into the network will be described, respectively. Lastly, a case study for a reduced Berlin scenario is conducted and impacts of PHEVs on the system are presented.

II. THE ENERGY HUB CONCEPT

The concept of “hybrid energy hubs”, where the term “hybrid” refers to facilitation of multiple energy carriers, is a generalization of a network node in interconnected power systems. It typically incorporates inputs, outputs, storages and numerous energy carrier conversions. The hub is defined through a hub equation consisting of load (**L**) and input (**P**) vector as well as hub coupling matrix (**C**) [11]. The general energy hub equation is shown in (1).

$$\underbrace{\begin{bmatrix} L_\alpha \\ L_\beta \\ \vdots \\ L_\omega \end{bmatrix}}_{\mathbf{L}} = \underbrace{\begin{bmatrix} c_{\alpha\alpha} & c_{\beta\alpha} & \cdots & c_{\omega\alpha} \\ c_{\alpha\beta} & c_{\beta\beta} & \cdots & c_{\omega\beta} \\ \vdots & \vdots & \ddots & \vdots \\ c_{\alpha\omega} & c_{\beta\omega} & \cdots & c_{\omega\omega} \end{bmatrix}}_{\mathbf{C}} \underbrace{\begin{bmatrix} P_\alpha \\ P_\beta \\ \vdots \\ P_\omega \end{bmatrix}}_{\mathbf{P}} \quad (1)$$

with

$$\alpha, \beta, \dots \in \mathcal{E} = \{\text{electricity, natural gas, hydrogen, } \dots\}$$

Here, $c_{\alpha\beta}$ denotes the coupling factor, consisting of the converter efficiencies transubstantiating energy carrier α to β . Further, L_α and P_α denote the load as well as power injection of energy carrier α , respectively. The hubs, which will be utilized in the system for analysis of PHEV impacts on interconnected multi energy carrier grids, are incorporating transformers, CHPs and furnaces. Further technologies can easily be integrated but, as the focus lies on PHEV integration, are omitted for system simplicity. The hub equation for all

nodes is denoted in (2), where $L_{m,e}^T$ is the electric load at hub H_m and time step T with $\eta_{m,ee}^{TR}$ being the transformer efficiency at hub H_m , respectively. Further, CHP and F specify the efficiencies of CHP and furnace and subscripts e , g and h denote electricity, natural gas and heat, respectively. A detailed derivation is found in [12].

$$\underbrace{\begin{bmatrix} L_{m,e}^T \\ L_{m,h}^T \end{bmatrix}}_{\mathbf{L}} = \underbrace{\begin{bmatrix} \eta_{m,ee}^{TR} & \nu_m^T \eta_{m,ge}^{CHP} \\ 0 & \nu_m^T \eta_{m,gh}^{CHP} + (1 - \nu_m^T) \eta_{m,gh}^F \end{bmatrix}}_{\mathbf{C}} \underbrace{\begin{bmatrix} P_{m,e}^T \\ P_{m,g}^T \end{bmatrix}}_{\mathbf{P}} \quad (2)$$

$\forall m \in \mathcal{H} = \{H_1, H_2, \dots, H_N\}$

III. PHEV MODELLING

PHEVs incorporate typical attributes of energy hubs, hence they can be also modelled through equation (1). In the past, this simplified approach was utilized to investigate the potential load which the cars would impose on the system. Typical outputs of the model have been battery level, tank level, miles driven, etc. [13]. However, for this paper the cars are supposed to arrive with battery levels distributed between 20% and 100% using an equipartition. They are assumed to connect in various areas, dependent on the daytime and their schedule. The exact behavior of the PHEV agents is simulated via MATSim (Multi Agent Transportation Simulation) [14], [15]. The PHEVs are then modelled as agents demanding energy in each area. Each agent has a nonlinear benefit function $B_k(SOC_k^T)$ and a total utility $u_k(q_k^T, SOC_k^T, \pi^T, \theta_k^T)$ denoted in equation (3). The utility of each agent is calculated by subtracting the energy costs from its benefit. Here, q_k^T denotes the acquired energy, SOC_k^T the state of charge, π^T the price signal and θ_k^T the personal valuation for acquired energy of agent k , respectively. It is obvious that the assigned energy q_k^T is dependent on the individual parameter θ_k^T in relation to all other valuations Θ^T of connected PHEV agents in T . The price which results from an optimization (see IV-A or [10]) is dependent on Θ^T , only.

$$u_k(q_k^T, SOC_k^T, \pi^T, \theta_k^T) = \theta_k^T B_k(SOC_k^T + q_k^T(\theta_k^T | \Theta^T)) - \pi^T(\Theta^T) q_k^T(\theta_k^T | \Theta^T)$$

with

$$B_k(SOC_k^T) = \alpha SOC_k^T - \beta (SOC_k^T)^2 \quad (3)$$

$\forall k \in \mathcal{PHEV} = \{phev_1, phev_2, \dots, phev_l\}$

The individual agents energy valuation θ_k is expressed by (4) where $DTime_k$, \overline{SOC}_k , SOC_k^T and Δt denote departure time in seconds, deliberated SOC at departure, current SOC and interval length in seconds (900s), respectively. Also, ϖ is the maximum transmittable energy by a plug in one hour weighted by the maximum battery energy content. It is expressed in terms of SOC. Variable τ is scaling factor. For increasing exponents x of the power function $\theta_{k,1}^T$, the agent's energy valuation becomes passive. In contrary, a more aggressive behavior incorporates the willingness to pay more for energy earlier during the day and is depicted in figure 1(a) [10].

$$\theta_{k,1}^T = 1 + \tau(T / (\frac{DTime_k}{\Delta t} - \frac{(\overline{SOC}_k - SOC_k^T)}{\frac{\varpi}{4} \eta_c}))^x$$

$$\theta_{k,2}^T = 1 + \tau \exp(-(\frac{DTime_k}{\Delta t} - \frac{\overline{SOC}_k - SOC_k^T}{\frac{\varpi}{4} \eta_c} - T)) \quad (4)$$

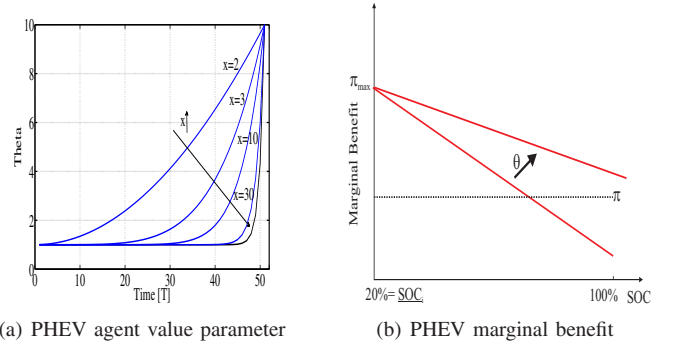


Fig. 1: Nonlinear pricing for PHEV agents. Agents personal value increases bidding curve over time. Maximal price of bidding curve is the weighted gasoline energy price

Furthermore, the agents will compete for energy in a bidding process when the location is overloaded due to limited converter capacities. The multiplication of the benefit function and the personal valuation can then, in some cases, lead to unaccountable bids, e.g. prices at hubs. This is restricted and avoided through the following reasoning. Agents will prefer to charge electricity as long as the price at the specific location is lower than the price of gasoline weighted by the conversion efficiencies. The maximal price can be calculated through (5), where π_{max} is the maximal price to be paid for electricity. The gasoline price is indicated by $\pi_{gasoline}$. Further, $\rho_{gasoline}$, η_{ICE} , η_{mot} , η_c and η_{dc} are energy density of gasoline, chosen to be 9.682 kWh/l [8], and the efficiencies for the ICE, the electric motor, battery charging and discharging, respectively. These values can be found in [13]. The maximum price for an electricity bid by an agent can be calculated to be 0.428 CHF/kWh, assuming a recent gasoline price of 1.5 CHF/l. The overall bidding behavior of the agents, represented by the marginal benefit, is depicted in fig 1(b) with a potential influence of θ_k . The lowest electricity price, without θ_k , at which the agents would still choose to recharge is set to 0.09 CHF/kWh, corresponding to the night tariff in Switzerland. The cars would then not recharge their batteries fully during the day since the tariff of 0.18 CHF/kWh is higher. However, the minimum can also be set to zero implying that agents will only recharge their batteries fully when the energy is for free. Note, that π_{max} in fig. 1(b) is related to SOC which implies a weighting factor to the maximal price, dependent on the maximum energy content of the particular battery.

$$\pi_{max} = \frac{\pi_{gasoline}}{\rho_{gasoline} \eta_{ICE}} \eta_{mot} \eta_c \eta_{dc} \quad (5)$$

IV. PHEV INTEGRATION INTO ENERGY HUB NETWORKS

Figure 2 displays the complete system under investigation. Here, the energy hub network consists of four buses, e.g. hubs represented by (2), interconnected through electricity and gas pipelines. Bus one is considered as the slack where electric and gas power are injected. Each node incorporates a base load. All areas feature sites where PHEVs can connect. Hence, management entities are integrated at all buses for

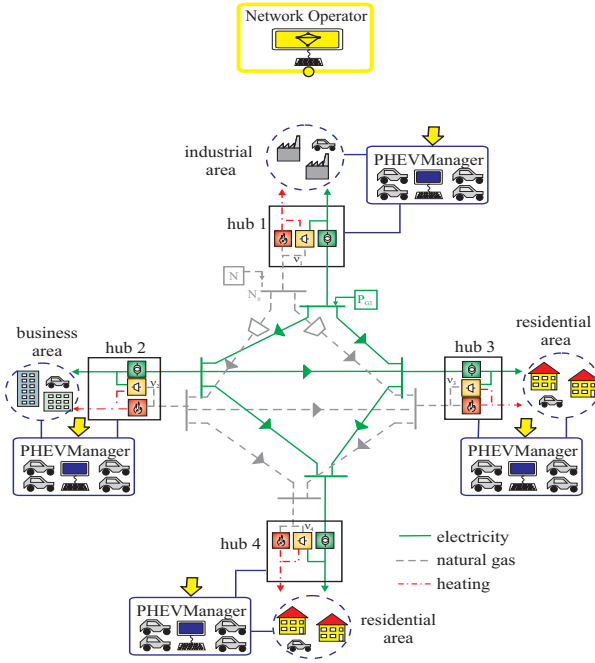


Fig. 2: Energy hub system integrating PHEV

PHEV integration. They are referred to as PHEV managers, dispatching available power in their area to connected vehicles. A network operator entity is installed, additionally. The operator is responsible for system security. It performs power flow calculations and intervenes as soon as one line is overloaded due to the current system state. The operator then triggers load reductions through a heuristic scheme and communicates updated, reduced, maximal PHEV load levels to the managers. This scheme fully integrates the managers into the network, circumventing possible insecurities based on excessive PHEV load. The manager updates its connectivity list every 15 minutes, hence the time steps of optimization and analysis are chosen commensurately.

A. The PHEV Manager

The manager was introduced and extensively elaborated on in [10]. In brief, the entity tries to recharge all PHEVs connected in its area supervised while maximizing their total utility in each time step. Clearly, the cars are connected to the hub via low voltage distribution lines which are not considered any further, here. The scheme, based on mechanism design [16] is denoted in its simplified version in (6), (7).

$$\text{Maximize} \quad \sum_{k \in \text{PHEV}} u_k(q_k^T, \text{SOC}_k^T, \pi^T, \theta_k^T) \quad (6)$$

$$\text{subject to} \quad 0 \leq q_k^T(\theta_k^T | \Theta^T) \leq \bar{q}_k^T \quad (7a)$$

$$\sum_{k \in \text{PHEV}} \varrho_k q_k^T(\theta_k^T | \Theta^T) \leq \Gamma^T \quad (7b)$$

$$\text{SOC}_k^T \leq 1 \quad (7c)$$

Variable $q_k^T(\theta_k^T)$ is the amount of energy which car k receives in time step T . It is bounded by the maximal amount of energy \bar{q}_k^T proportional to the maximal power connection (3.5kW) and expressed in terms of maximal SOC_k . The sum

of all individual, weighted energy consumptions multiplied by the respective maximum battery energy contents ϱ_k is bounded by the maximal transferable energy via transformer and CHP, denoted here by Γ^T . Also, the respective SOC is bounded in each time step to be lower or equal 100%.

The maximal amount of available energy to be dispatched is calculated by the manager according to (8) and based on the electric- as well as heat base load. The variable \bar{P}_{me} corresponds to the maximal electricity input of the transformer. It is divided by the transformer efficiency in order to attain the maximally allowed transformer loading. The other values have been introduced before. Once the total PHEV energy Γ^T has been calculated through the manager, it is used to adjust the base load at the node by adding Γ^T/ζ to the base electricity load L_{me}^T as shown in (9). The variable ζ introduces the hourly fraction of the chosen interval, here $\frac{1}{4}$. However, Γ^T not necessarily equals Γ^T . The sum \hat{L}_{me}^T is then used by the central network operator for power flow calculations. Note that the base load has a higher priority as the PHEVs as will be shown later.

$$\Gamma^T = \left(\frac{\bar{P}_{me}}{\eta_{TR}^{ee}} + \frac{L_{me}^T h \eta_{mge}^{CHP}}{\eta_{mgh}^{CHP}} - L_{me}^T \right) \zeta \quad (8)$$

$$\hat{L}_{me}^T = L_{me}^T + \frac{\Gamma^T}{\zeta} \quad (9)$$

B. The Energy Hub Network

Here, the hubs are assumed to represent substations at a high voltage level (e.g. 110 kV). Hence, a simplifying DC-model, incorporating maximum line capacities, can be chosen to model electricity lines [17], [18] and investigate possible, rudimentary repercussions on the power grids from large scale PHEV utilization. Voltage levels and reactive power consumption at the nodes are not considered. Gas networks can basically be modelled in the same way as power networks using gas nodal balance- (10) and line equations (11), (12), respectively. Network nodes are denoted as the set \mathcal{N} , considering $N_{\mathcal{N}}$ as the total number of nodes in the system also referring to the number of hubs \mathcal{H} .

$$F_{mg} - \sum_{n \in \mathcal{N}/\{m\}} F_{mng} = 0 \quad (10)$$

$$\forall m \in \mathcal{N} = \{1, 2, \dots, N_{\mathcal{N}}\}$$

In (10), F_{mg} is the volume flow injected at node m . Flows between nodes can be expressed as functions of the upstream and downstream pressures p_m and p_n as in (11) and (12). Properties of the pipeline and the fluid are represented by the constant k_{mn} [19], chosen here between 2 and 6 in order to model various pipeline lengths.

$$F_{mng} = k_{mn} s_{mn} \sqrt{s_{mn} (p_m^2 - p_n^2)} \quad (11)$$

where

$$s_{mn} = \begin{cases} +1 & \text{if } p_m \geq p_n \\ -1 & \text{else} \end{cases} \quad (12)$$

The generation of pressure through compressors needs power. Presuming that the compressor is driven by a gas turbine, the corresponding power consumption can be considered

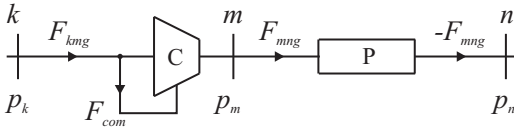


Fig. 3: Model of transmission link with compressor (C) and pipeline (P).

as additional power flowing into the pipeline section, depicted in figure 3. The amount of power consumed by the compressor depends on the pressure added to the fluid and the volume flow rate through it. Using the notation of figure 3 the compressor demand can be approximated with

$$F_{com} = k_{com} F_{mng} (p_m - p_k) \quad (13)$$

where k_{com} is a constant characterizing the compressor unit; p_k and p_m are the suction and discharge pressures, respectively [19], [20].

The volume flow rate F_{mng} between nodes m and n corresponds to power flow P_{mng} . The relation between volume and power flow is given by

$$P_{mng} = GHV \cdot F_{mng} \quad (14)$$

where GHV is the gross heating value of the fluid.

In figure 2, potential electric power flows in the lines are represented by the green arrows, whereas gas flows are indicated by grey arrows. A detailed model for interconnected energy hubs using also an AC-power line model can be found in [12]. Table I gives an overview of the assumptions for each hub i .

symbol	value	description
η_{e}^{TR}	0.98	transformer coupling
η_{g}^{CHP}	0.35	CHP coupling
η_{g}^{CHP}	0.45	CHP coupling
η_{g}^h	0.75	furnace coupling
π_e	9, 18 Rp/kWh	electricity price
π_g	11 Rp/kWh	natural gas price
\bar{P}_{TR}	2 p.u.	upper transformer limit
\underline{P}_{TR}	-2 p.u.	lower transformer limit
\bar{P}_{CHP}	0.5 p.u.	upper CHP limit
\underline{P}_{CHP}	0 p.u.	lower CHP limit
\bar{P}_F	5 p.u.	upper furnace limit
\underline{P}_F	0 p.u.	lower furnace limit

TABLE I: Energy hub assumptions

C. Multi Step Optimization through the network operator

The optimization of the system is carried out on two levels and for multiple time steps. On the lower level, the managers first update their respective PHEV lists for the actual time step. Using the lists, they individually maximize total agent utility for each hub, e.g. area, according to the scheme described earlier in IV-A. On the higher level, the network operator minimizes total system costs while supplying the system and PHEV load, fulfilling system constraints on power flows. Prices for various energy carriers are multiplied by system infeeds for calculation of system costs and are plotted in figure 4. They reflect actual energy prices in Switzerland for electricity (high- and low price tariffs over the day) and gas (1 Rp = 0.0086

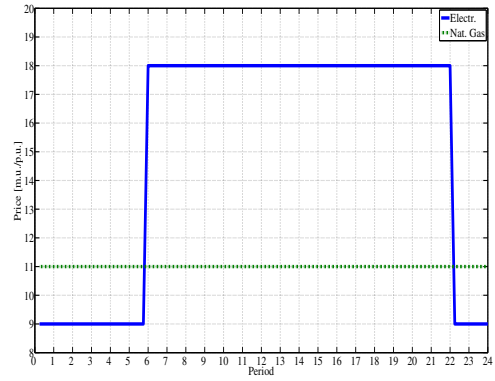


Fig. 4: Energy prices (electricity, gas) for one day, e.g. 24h

US cents), denoted in table I. In the figure, they are given in monetary units incorporating scaling factors. The network optimization scheme is denoted in equations (15)-(17). The objective function is dependent on the total consumption of energy carriers. The equality constraints consist of the hub and the network power equations, latter represented by \mathbf{G}_α . These are generally nonlinear and part of them is formulated in (10)-(14). The rest can be found elsewhere [18]. Inequality constraints refer to hub power inputs \mathbf{P}_i , converter inputs \mathbf{P}_{ci} , network carrier flows \mathbf{F}_α as well as dispatch factors \mathbf{N}_i . These calculations are repeated for every time step T as the amounts of PHEVs and their preferences for energy acquisition change in time. Apart from these modifications the same formulations for system optimization are chosen as in [12], [20].

Minimize

$$f(\mathbf{P}_i^T) \quad (15)$$

subject to

$$\mathbf{L}_i^T - \mathbf{C}_i \mathbf{P}_i^T = \mathbf{0} \quad \forall i \in \mathcal{H} \quad (16a)$$

$$\mathbf{G}_\alpha^T (\mathbf{P}_i^T) = \mathbf{0} \quad \forall \alpha \in \mathcal{E} \quad (16b)$$

and

$$\underline{\mathbf{P}}_i \leq \mathbf{P}_i^T \leq \bar{\mathbf{P}}_i \quad \forall i \in \mathcal{H} \quad (17a)$$

$$\underline{\mathbf{P}}_{ci} \leq \mathbf{N}_i^T \mathbf{P}_i^T \leq \bar{\mathbf{P}}_{ci} \quad \forall i \in \mathcal{H} \quad (17b)$$

$$\underline{\mathbf{F}}_\alpha \leq \mathbf{F}_\alpha^T \leq \bar{\mathbf{F}}_\alpha \quad \forall \alpha \in \mathcal{E} \quad (17c)$$

$$\mathbf{0} \leq \mathbf{N}_i^T \leq \mathbf{1} \quad \forall i \in \mathcal{H} \quad (17d)$$

Restricted by their areal optimization, the PHEV managers could cause network problems. In situations where the electric grid is already heavily loaded, line constraints could be violated since the managers could impose an excessive load to the network as a whole. Managers, when acting, only consider their local situation (transformer loading) but do not take into account any loadings of in- and outgoing power lines or the complete system state, e.g. loads at other buses. Therefore, technical bounds of the transformers can be met lines could become overloaded. In order to counteract such insecurities, a simple heuristic for load shedding is implemented into the central network control, assuring the flexibility and applicability of the PHEV management system. The network control sends signals to adjust loads at the right buses in right

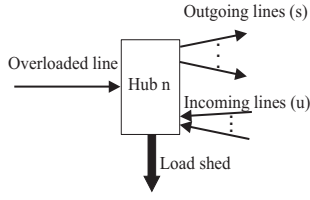


Fig. 5: Partial overloaded network

amounts, averting overloads. Load curtailment focusses only on PHEVs. In fact, these vehicles are a controllable, uncritical load since all of them incorporate an auxiliary power source. The heuristic can be found in [21], [22] and is simplified due to the chosen approach of load and electric power line modelling. Figure 5 depicts an insecure situation in a part of a network. The network control analyzes the situation and sheds excessive PHEV load based on the following scheme being formulated in (18):

- 1) The overloaded branch is identified.
- 2) The direction of the overload is found, e.g. the receiving bus (here n).
- 3) All neighboring, receiving buses (s) connected via branches of outgoing power are identified.
- 4) The excessive load ΔP_{exc} in the overloaded branch is calculated.
- 5) 50% of ΔP_{exc} are shed at the receiving bus (Hub n)
- 6) $\frac{50\%}{s}$ of ΔP_{exc} are equally shed at all other buses found in step 3.

In the formulation of (18) the variable $\Delta P_{exc mn}^T$ denotes the excessive power on the branch between bus m and n in time step T . It is calculated by subtracting the maximally transferable power \bar{P}_{mn} of that branch from the calculated line flow P_{mn}^T . In order to relieve the overloaded line, 50% of the excess power is shed in the receiving bus ($P_{LS n}^T$). The rest is shed equally at all other receiving buses s connected to bus n ($n \neq q$ where $P_{nq}^{T r} > 0$), denoted by the sum in (18b).

$$\Delta P_{exc mn}^T = P_{mn}^T - \bar{P}_{mn} \quad (18a)$$

$$\Delta P_{exc mn}^T = P_{LS n}^T + \sum_{q \neq n} P_{LS q}^T \quad (18b)$$

$$P_{LS n}^T = 0.5 \Delta P_{exc mn}^T \quad (18c)$$

$$P_{LS q}^T = \frac{0.5}{s} \Delta P_{exc mn}^T \quad \forall q \neq n \wedge P_{nq}^{T r} > 0, r = 1 \dots s \quad (18d)$$

V. BERLIN CASE STUDY AND RESULTS

The system introduced in the precedent paragraphs is used to model a 1% Berlin (inner city) scenario based on MATSim simulations delivering transportation data in an equilibrium. Hence, it exhibits a real life situation for all agents concerning their daily schedules. A number of 15931 PHEV agents is utilized to picture a small scale setting of actual driving and parking behavior in cities. For future considerations of large scale transportation scenarios, millions of agents could be integrated and managed through this system. Here, the complete city is modelled via 6941 links, each representing

a street. The agents are able to park in those streets, assuming pervasive connections to the power network. The agents connect with a randomly chosen SOC (between 20% and 100%). The links in close vicinity to each other are assigned to one hub. Each hub contains several hundreds of links, however, the biggest includes roughly 4700 whereas the smallest 250. It is easily imagined that with detailed information about the power supply architecture of a city, a tailored hub model could represent an even more realistic situation.

Most of the agents start fully charged at their home location and drive to their work places in the morning. However, some of them also move between links and therefore partly between hubs, imposing and shifting the load from one hub to the other. Note, that connection points are assumed to be everywhere. For investigations of PHEV impacts, the system is simulated in a base case with no PHEV penetration. In a second simulation the described agents are integrated and effects on the system are studied.

A. Base case

The system without PHEVs includes electric and heat loads (blue (b), solid) for all hubs, which are depicted in fig. 6(a)-(h). For interpretational simplicity and visibility the loads are kept identical at all hubs. Generally, the electric inputs (green (g), dashed) at hubs are bigger than loads as in fig. 6(b), (c), 6.00h-22.00h. This applies also to the heat loads in fig. 6(e)-(h) and is due to the converter efficiencies being lower than one. It can also easily be seen that for some hubs, for instance hub 1 in fig. 6(a), the shape of the electric input does not relate to the load in time steps 6.00h-22.00h.

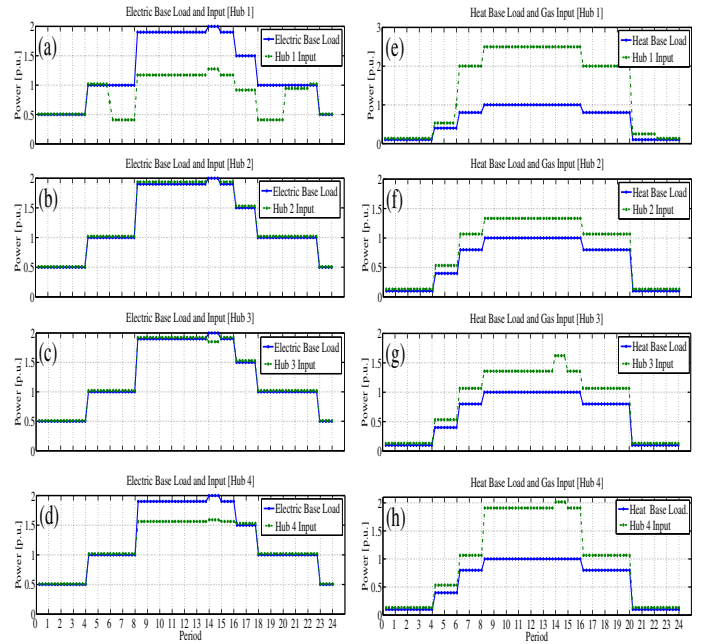


Fig. 6: Base loads + inputs (el., gas), hubs 1-4 (24h)
(a)-(d) Electric base load (b, solid), input (g, dashed)
(e)-(h) Heat base load (b, solid), nat. gas input (g, dashed)

This is justified in the utilization of the CHPs (see increased gas input for hub 1 fig. 6(e)), the respective line loadings

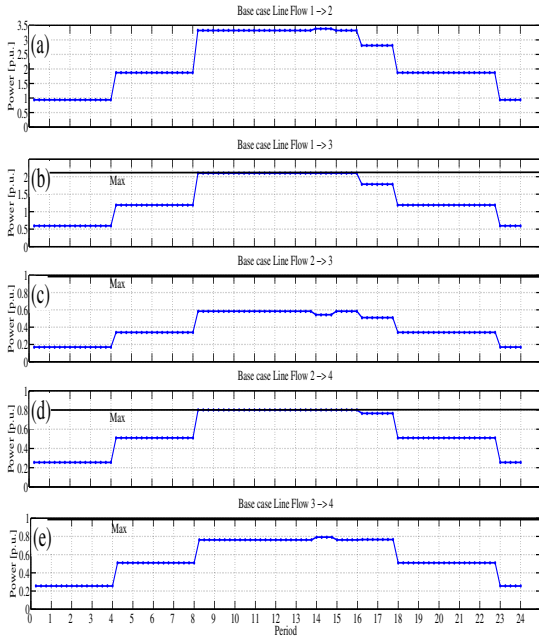


Fig. 7: Line flows in base case (24h)

and energy prices. The CHP in hub 1 is switched on during periods 6.00h-22.00h because the gas price is much lower than the electricity price, as displayed in fig. 4. At this hub, it is more profitable to use the CHP during the high price tariff. However, the other hubs do not generate electricity through this converter. Evidently, the compressors would need to be used more heavily, creating losses due to inefficiencies, not compensated by the lower gas price. Later in the day, CHPs at other hubs are used for conversion since electricity lines are fully loaded and no more electric power can be delivered to the respective hubs. This can be observed comparing figure 6 and figure 7. Between 8.00h and 16.00h lines 1→3 and 2→4 are fully loaded. This is also the time interval during which the CHPs at hub 3 and at hub 4 are switched on as observable in the increased natural gas consumption in 6(c),(d). The converter compensates for the shortcomings of the network and supplies the part of the load that cannot be met by the electricity network. Obviously, the system situation represents a worst case scenario for future PHEV integration since additional load would even more stress the system state.

B. PHEV case

The PHEVs are presumed to start fully loaded at their starting locations (e.g. home) in the morning and arrive at their destinations with randomly discharged battery levels. Obviously, with pervasive connection points, a large load is found to be imposed in the morning hours. In fact, the agents do not bother to recharge even during high price times, as the electricity price weighted by converter efficiencies is always lower as the gasoline price they would otherwise pay. This PHEV load stresses the system even more and leads to infeasible solutions of the power flows, as lines, that were already fully loaded in the base case, become overloaded. Evidently, the capacities are violated as visualized in 8(b) and

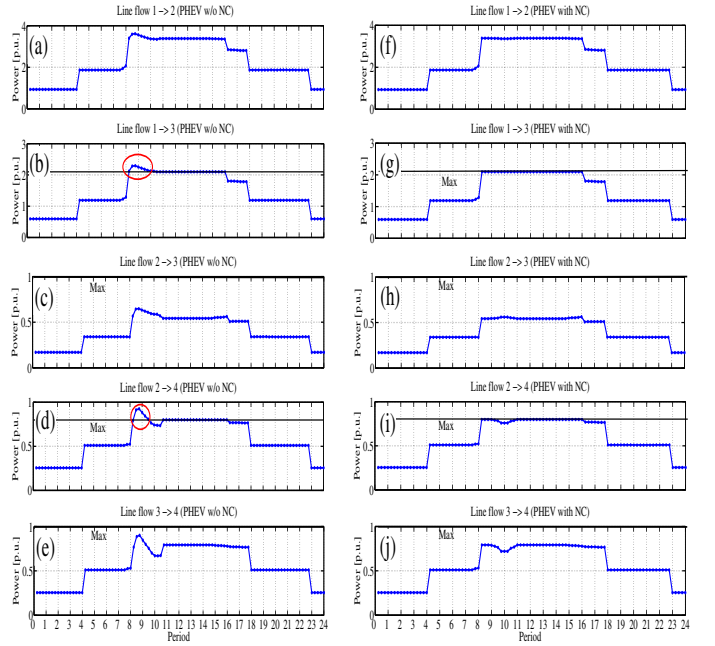


Fig. 8: Line flows (PHEV case) without/with network control
 (a)-(e) Line flows without network control (capacity violations circled)
 (f)-(j) Line flows with network control (no capacity violations)

(d) during 8.00h and 9.30h by the circled areas. The maximum capacity of each line is denoted by the horizontal line and indicated by "Max". The system becomes insecure and switches could be utilized to cut off lines. Here, the network control communicates load reductions to particular PHEV managers which are determined by the heuristic. These entities shed the amount of load calculated via (18), resulting in less PHEVs recharging. The system optimization is then repeated until the line flows are within their bounds. Figure 8(f)-(j) visualizes the results after repeated usage of the heuristic. Clearly, all lines are within their technical constraints and potential line tripping is avoided.

The system optimization including the network control leads to the hub loads and inputs depicted in figure 9. Clearly, the heat loads do not change as the cars only have an impact on electricity consumption. Therefore, the electric load changes and variations differ from hub to hub. Evidently, hub 1, including the most links, congests relatively fast and for the time between 8.00h and 16.00h as seen in figure 9(a). Due to the fact that all hubs are heavily loaded in the late morning hours and throughout the day, depicted in fig. 6(a)-(d), the PHEV load is mitigated to later hours as already shown in [10] and displayed best in fig. 9(a). The PHEV manager's optimization scheme thereby assures that the transformer bound is not violated and found to be 2p.u. at all times. Note that the PHEVs are arriving and leaving due to their day schedule on a constant basis, as simulated via MATSim.

In order to supply as many PHEVs as possible, additional electric power generation from CHPs is used according to (8). These converters are used more intensively as in the base

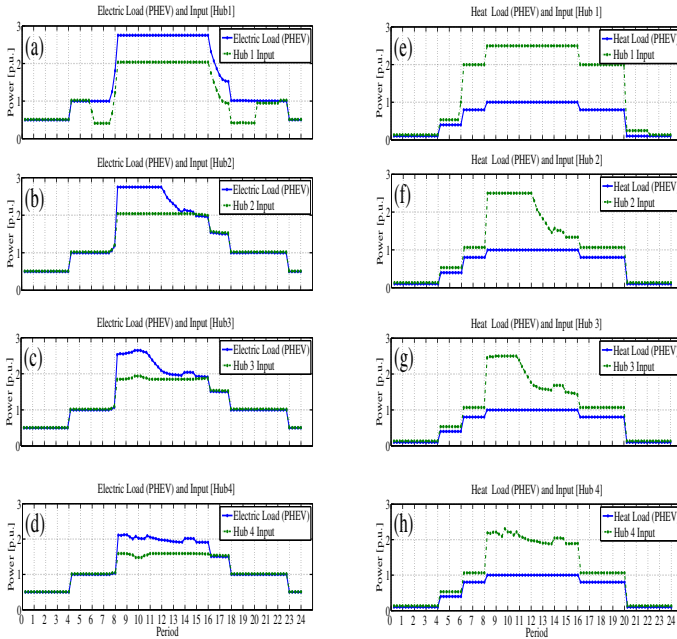


Fig. 9: Loads + inputs incl. PHEVs (el., gas), hubs 1-4 (24h)
 (a)-(d) Electric load (b, solid), input (g, dashed)
 (e)-(h) Heat load (b, solid), nat. gas input (g, dashed)

case, so the natural gas input to the hubs, e.g. the power input from gas, is increasing. This can be observed in figures 9(e)-(h) (green, dashed). Comparing these inputs to the base case of figures 6(e)-(h), it can easily be noticed that hub 1 behaves similarly as in the the base case but all other hubs exhibit increased natural gas facilitation. It is straightforward to perceive the connection between the additional gas input and the production of electricity as the shape of the gas inputs clearly refers to the increased and mutated levels of electric power demands, displayed in figures 9(a)-(d) (blue, solid). Plots of the dispatch factors N_i verify this but cannot be shown due to space limitations.

Furthermore, in cases were the maximum of potentially supported PHEV load is not reached by electric inputs and gas conversion is utilized to a substantial amount, the reasoning is found by looking at the system situation. In figures 9(c) and (d), it is noticed, that the electric load is bigger than 2p.u. but the electric inputs of both hubs are less, not fully utilizing the possibilities to supply PHEVs with efficiently converted power. The electricity supply is substituted by increased CHP production. This can be explained by the congestion of the electric lines connecting those hubs. Evidently, the lines 1→3 and 2→4 are fully loaded, even after the heuristic based load shedding and no more electric power can be delivered to hub 3 and hub 4. As the scheme always tries to recharge as many PHEVs as possible and the electric input to the transformer is limited by the connected lines, the rest of the load is simply supplied by the CHPs. However, the maximal electric output of these converters is bounded by the heat demand of the hub.

Evidently, when the power input to particular hubs is congested, the agent's bidding process for energy results into rising energy prices. This process presumes that PHEV agents

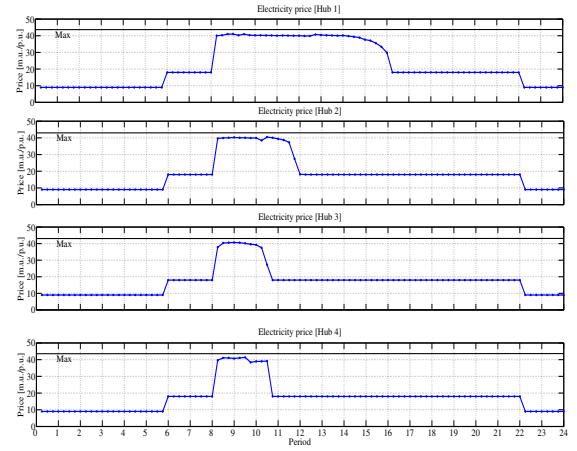


Fig. 10: Electricity prices for PHEVs at hubs (24h). Maximal price (π_{max} from (5)) equivalent to weighted gasoline price is marked

would like to be fully recharged when leaving the location. The rising prices assure a disqualification process for agents incorporating less interest for being recharged than others. The behavior has been described in (3) and figure 1 as well as in [10]. The resulting electricity prices are plotted in figure 10 for all hubs. The price for electricity is increased substantially during congested times. Clearly, the maximal price for electric energy stays lower than the earlier computed, weighted gasoline price (42.8 m.u./p.u.) at all hubs. Hub 1 is congested the longest, whereas hubs 3 and 4 experience the shortest congestion times. The different tariff intervals can also be perceived. However, a constant price later in the day does not necessarily express that no PHEVs are recharged in the system, it just exhibits no noticeable congestion. Examples are observed in figures 9 (b)-(d) and figures 10(b)-(d) between 11.00h-14.00h. In fact, the presented prices can as well be regarded as a control signal. They do not necessarily reflect actual hub- e.g. nodal prices. However, the network friendly controllability of the PHEVs directly relates to this incentive signal presuming that the agents act rational e.g. are equipped with a smart charger.

Note that the congestion of the system only appears during day times. Night charging is not specifically investigated here as the system is generally less stressed. The input from MAT-Sim also does not incorporate charging at the home locations yet. Only recharging at working and shopping locations is considered. This is observed in fig. 9 as the load shape in the evening hours is almost not mutated and variations are barely seen. However, extending the system to include more links, hubs, night time charging and particularly more agents would lead to noticeable variations of hub evening load patterns.

VI. SUMMARY

This paper introduces PHEVs as agents into energy hub networks. Simulations of driving behavior are carried out and numerous variations of connection times, locations and battery levels are used as inputs for power system simulations. Smart entities manage PHEV demand dependent on current energy carrier prices, converter and line limits at different locations

and times avoiding violation of system constraints. Changes of hub loads, line flows, converter utilization degrees and prices paid by PHEVs are studied and ramifications are analyzed.

A. Shortcomings

At the current development stage, the investigated system does not consider reactive power flows by using only a DC-model of the network. Voltage levels and stability as well as detailed modelling of lower network levels are not assessed. This needs to be integrated to further perceive possible impacts of large scale PHEV usage. Also, losses and system services from PHEVs are not considered. Detailed data on daily loads, line capacities and system architecture is also not utilized and night time charging is missing.

B. Conclusions and Future Work

The scheme paves the way to a fully integrated power and transportation system. New load profiles can be assessed and the utilization of distributed generation proves the viability to supply increased demand from PHEVs. Furthermore, control schemes based on market algorithms can be used to distribute converter limited energy resources efficiently between PHEVs. The scheduling of the participants also includes assessment of system security as higher level controllers are able to exert influence on the distributed management entities of vast numbers of PHEVs. The future work will tackle the shortcomings, model PHEVs in distribution grids and investigate their usage for renewable energy generation expansion.

VII. ACKNOWLEDGEMENTS

The work is sponsored by the Swiss Federal Institute of Technology (ETH) Zurich under research grand TH 2207-3 and by the Swiss Federal Office of Energy. It is carried out within the framework of the research project Vision of Future Energy Networks. The author would like to thank all colleagues and especially Rashid Waraich from the Institute for Transport Planning and Systems (IVT) at ETH Zurich.

REFERENCES

- [1] B. D. Williams and K. S. Kurani. Commercializing light-duty plug-in/plug-out hydrogen-fuel-cell vehicles: "mobile electricity" technologies and opportunities. *Journal of Power Sources*, 166(2):549–566, 2007.
- [2] M. J. Scott, M. Kintner-Meyer, D. B. Elliot, and W. M. Warwick. Impacts assessment of plug-in hybrid electric vehicles on electric utilities and regional u.s. power grids, economic analysis. In *10th Annual EUEC Conference*, pages 1–19, Tucson, AZ, USA, 2007. Pacific Northwest National Laboratory (PNNL).
- [3] H. Turton and F. Moura. Vehicle-to-grid systems for sustainable development: An integrated energy analysis. *Technological Forecasting and Social Change*, 75:1091–1108, 2008.
- [4] P. Denholm and W. Short. An evaluation of utility system impacts and benefits of optimally dispatched plug-in hybrid electric vehicles. Technical report, National Renewable Energy Laboratory (NREL), 2006.
- [5] J. Tomic and W. Kempton. Using fleets of electric-drive vehicles for grid support. *Journal of Power Sources*, 168(2):459–469, 2007.
- [6] S. W. Hadley. Evaluating the impact of plug-in hybrid electric vehicles on regional electricity supplies. In *Bulk Power System Dynamics and Control*, Charleston, SC, USA, 2007.
- [7] K. Schneider, C. Gerkenmeyer, M. Kintner-Meyer, and R. Fletcher. Impact assessment of plug-in hybrid electric vehicles on pacific northwest distribution systems. In *IEEE Power and Energy Society 2008 General Meeting*, pages 1–6, Pittsburgh, Pennsylvania USA, 2008.

- [8] C. Roe, J. Meisel, F. Evangelos, T. Overbye, and A. P. Meliopoulos. Power system level impacts of phev. In *42nd Hawaii International Conference on System Sciences, 2009. HICSS '09.*, pages 1–10, 2009.
- [9] X. Yu. Impacts assessment of phev charge profiles on generation expansion using energy modeling system. In *IEEE Power and Energy Society 2008 General Meeting*, Pittsburgh, Pennsylvania, USA, 2008.
- [10] M. D. Galus and G. Andersson. Demand management for grid connected plug-in hybrid electric vehicles (phev). In *IEEE Energy 2030*, pages 1–8, Atlanta, GA, USA, 2008.
- [11] M. Geidl, G. Koepfel, P. Favre-Perrod, B. Kloockl, Andersson G., and K. Froehlich. Energy hubs for the future. *IEEE Power and Energy Magazine*, 5(1):24–30, 2007. 1540-7977.
- [12] M. Geidl and G. Andersson. Optimal power flow of multiple energy carriers. *IEEE Transactions on Power Systems*, 22(1):145–155, 2007. 0885-8950.
- [13] M. D. Galus and G. Andersson. Power system considerations of plug-in hybrid electric vehicles based on a multi energy carrier model. In *Power and Energy Society (PES) General Meeting*, Calgary, Canada, 2009.
- [14] M. D. Galus, R. Waraich, M. Balmer, K. W. Axhausen, and G. Andersson. A framework for investigating the impacts of plug-in hybrid electric vehicles. In *International Advanced Mobility Forum (IAMF)*, Geneva, Switzerland, 2009.
- [15] M. Balmer, K. Meister, M. Rieser, K. Nagel, and K.W. Axhausen. Agent-based simulation of travel demand: Structure and computational performance of matsim-t. In *2nd TRB Conference on Innovations of Travel Modeling*, Portland, OR, USA, 2008.
- [16] M. Fahrioglu and F. L. Alvarado. Designing incentive compatible contracts for effective demand management. *IEEE Transactions on Power Systems*, 15(4):1255–1260, 2000. 0885-8950.
- [17] J. W. Wood and F. B. Wollenberg. *Power generation, operation and control*. Wiley-Interscience, 2nd edition, 1996.
- [18] A. J. del Real, M. D. Galus, C. Bordons, and G. Andersson. Optimal power dispatch of energy networks including external power exchange. In *European Control Conference (ECC) 09*, pages 1–6, Budapest, Hungary, 2009.
- [19] K. F. Pratt and J. G. Wilson. Optimization of the operation of gas transmission systems. *Transactions of the Institute of Measurement and Control*, 6(5):261–269, 1984.
- [20] M. Geidl. *Integrated Modelling and Optimization of Multi-Carrier Energy Systems*. PhD thesis, ETH, 2007.
- [21] S. Shah and S. M. Shahidehpour. A heuristic approach to load shedding scheme. *IEEE Transactions on Power Systems*, 4(4):1421–1429, 1989. 0885-8950.
- [22] Zhao Yuan, Zhou Nianchen, Zhou Jiaqi, Xie Kaigui, Liu Yang, and Kuang Jun. A heuristic approach to local load shedding scheme for reliability assessment of bulk power systems. In *IEEE/PES Transmission and Distribution Conference and Exhibition: Asia and Pacific*, pages 1–5, 2005.



Matthias D. Galus was born in Swientochlowitz, Poland. He received a Dipl.-Ing. degree in electrical engineering and a Dipl.-Ing. degree in industrial engineering from the RWTH Aachen, Germany, in 2005 and in 2007, respectively. He joined the Power Systems Laboratory of ETH Zurich, Switzerland in 2007 where he is working towards a PhD. His research is dedicated to modeling, optimization and efficient integration of PHEV into power systems. He is a student member of the IEEE and VDE (German society of electrical engineers).



Göran Andersson was born in Malmö, Sweden. He obtained his MSc and PhD degree from the University of Lund in 1975 and 1980, respectively. In 1980 he joined ASEA, now ABB, HVDC division in Ludvika, Sweden, and in 1986 he was appointed full professor in electric power systems at the Royal Institute of Technology (KTH), Stockholm, Sweden. Since 2000 he is full professor in electric power systems at ETH Zurich, Switzerland, where he heads the Power Systems Laboratory. His research interests are in power system analysis and control, in particular power system dynamics and issues involving HVDC and other power electronics based equipment. He is a member of the Royal Swedish Academy of Engineering Sciences and Royal Swedish Academy of Sciences and a Fellow of IEEE.

ular power system dynamics and issues involving HVDC and other power electronics based equipment. He is a member of the Royal Swedish Academy of Engineering Sciences and Royal Swedish Academy of Sciences and a Fellow of IEEE.